European Rotorcraft Forum

# SIMULATION OF A COMPOUND-SPLIT TRANSMISSION FOR THE UH-60

P. Paschinger, pierre.paschinger@tuwien.ac.at, Zoerkler Gears GmbH & Co KG (Austria)
M. Weigand, michael.weigand@tuwien.ac.at, Technische Universität Wien (Austria)

**Abstract**
Recent studies showed that the variation of the main rotor speed of the Sikorsky UH-60 (Black Hawk) offers the opportunity to reduce the propulsive power demand significantly in some flight states. A possibility to achieve this goal without changing the speed of the two turboshaft engines is the use of a Continuously Variable Transmission (CVT). One possible implementation is a so-called Compound-Split (CS), a special type of power-split transmission. The aim of this study is to present a drivetrain architecture of this type for the UH-60 helicopter and to show the feasibility by performing simulations in the time-domain. The results show that the transmission system is able to transmit the power in all searched flight conditions and the main rotor speed is kept within narrow limits around the target values.

## NOMENCLATURE

| | |
|---|---|
| $\alpha$ | angle of attack |
| $\Theta$ | mechanical point (MP) |
| $\vartheta$ | control angle |
| $\Phi$ | transmission spread |
| $\Psi$ | azimuth angle |
| $\Omega$ | angular velocity of main rotor in rad/s |
| $\omega$ | angular velocity in rad/s |
| $b$ | face width |
| CS | Compund-Split |
| $d_w$ | working pitch diameter |
| $i_{12}$ | planetary ratio of a planetary gear set |
| $k_{ab}$ | speed ratio of shafts $a$ and $b$ (basic ratio) |
| $n$ | rotational speed in RPM |
| $n_{\max}$ | maximum RPM of a hydraulic machine |
| $P$ | power |
| $P_{\text{corner}}$ | corner power of a hydraulic machine |
| $P_{\max}$ | maximum power of a hydraulic machine |
| $q$ | number of planets of a planetary gears set |
| $T_{\max}$ | maximum torque of a hydraulic machine |



## 1. INTRODUCTION

### 1.1. State of research

Several studies have shown, that variation of the main rotor speed of the Sikorsky UH-60 offers the opportunity to reduce power demand as well as fuel consumption in some flight states. Mistry and Gandhi[20] found that a power reduction up to 12 % is possible. Misté et al.[19] presented a methodology for determining the optimal rotational speed of the main rotor and showed that more than 10 % fuel saving is feasible. Furthermore, the rotor-turboshaft integration was examined and fixed-ratio transmissions were compared to continuously variable transmissions (CVT)[17,18]. Garre et al.[12] confirmed these results and stated that within a range of 70 % to 110 % of nominal main rotor speed, power reductions of up to 15 % can be achieved.

Different solutions to realize a variable rotor RPM have been published, inter alia Variable-Speed Power-Turbines (VSPT)[34,29,16] and transmission systems with variable ratio[2]. Amri et al.[1] compared the different approaches and found a variation of rotor speed by means of the transmission system the most preferable solution. Based on this, CVTs were determined as the best option for meeting

the requirements of helicopters with variable rotor speed and Compound-Split (CS) transmission was proposed for usage in rotorcraft[23].

### 1.2. Compound-Split transmission

A Compound-Split transmission is one of several possible implementations of a power split transmission system. The input power of a main (thermal) engine is split up into a mechanical and a so-called variator path. This kind of transmission system is known from hybrid electric vehicles. However, no power source other than the thermal engine is needed. Thus, it can be used as a continuously variable transmission (CVT). In principle, it comprises two nested epicyclic gear sets. Two of the three shafts of each epicyclic gear set are connected, which leads to two kinematic degrees of freedom of the resulting system. The variator is built up by two machines transforming mechanical power into another form, one operating as generator and the other as motor. The output speed is determined by the speed of the input shaft (main engine) and the transmission ratio of the variator.[15,23]

## 2. A COMPOUND-SPLIT TRANSMISSION SYSTEM FOR THE UH-60

In this section, a principle layout of a transmission system containing Compound-Split modules is presented. The basic approach was to keep as much of the baseline drivetrain[30] as possible unchanged to avoid issues with systems of the rotorcraft and to limit the scope of the study. A detailed description of the assumptions and decisions leading to the proposed design is given in a previous publication of the authors[24]. The most important points are:

1. Based on a study on the influence of variable main rotor speed on the operation of the tail rotor[8], it was decided to keep TR speed constant and thus independent of MR speed.

2. To avoid issues with the high-speed input bevel gear stage, the free-wheeling unit and the accessories, these parts of the drivetrain are kept as they are in the proven baseline transmission system.

3. For reasons of reliability of the system, it was decided to use two CS modules, one in the power path of each turboshaft engine.

4. Because of the high masses expected for electric machines for the variator, it is focussed on hydraulic transmission.

The resulting drivetrain architecture is depicted in figure 7 in appendix A.1. We give a short description, following the power path from the turboshaft engines to the main rotor. As stated in assumption 2, the parts comprising the turboshaft engines, free-wheeling units and accessories (not shown) are not changed compared to the baseline drivetrain. The first important change is that the tail rotor take-off is arranged immediately after the free-wheeling units on each side of the rotorcraft. From there, the TR power is transmitted to a combining bevel gear stage and further to the TR (*green*), which rotates at $1090\,\mathrm{RPM}$ (*pink*).

The following parts of the drivetrain are the CS-modules, which transform the input speed of $5750\,\mathrm{RPM}$ into a variable output speed of $2950\,\mathrm{RPM}$ to $4425\,\mathrm{RPM}$, corresponding to a transmission spread of $\Phi = 1.5$. This value was chosen based on the finding that a variation between $70\,\%$ to $110\,\%$ of the baseline MR speed is desirable[12]. Each CS-module consists of two nested epicyclic gear sets, labelled **C** and **D**, and the variator. The input and output shafts of the variator are connected to the epicyclic gear sets via helical gear stages with transmission ratios $i_c$ and $i_d$. The ring gear of **C** is driven by the input shaft of the CS-module. The sun gears of both EGS are connected via a shaft (*blue*) and the carrier of **C** along with the ring gear of **D** form the output shaft (*red*). The variator pump is connected to the two sun gears while the motor drives the carrier of EGS **D**.

After being transformed, the propulsive power of each turboshaft engine is transmitted to a combining bevel gear stage similar to the one in the baseline drivetrain and further to a planetary gear set and the main rotor (*dark green*).

The basic design data of the proposed transmission system is summarized in table 1. Where applicable, the numbers of teeth of the gears in the baseline design are compared to the ones in the variable-ratio drivetrain. To obtain an estimation of the mass and inertia of the transmission system, working pitch diameters and face widths of the gears are specified in the two columns on the right. These values are based on published data of the baseline drivetrain[22,21,10] respectively estimated based on standard calculation procedures for gears (current versions of ISO 6336 and ISO 10300). Following a convention, numbers of teeth and diameters of ring gears have a negative sign.

The input bevel gear stage is kept unchanged. The numbers of teeth of the gears of the CS modules were determined such that the required mechanical points[24] of $\Theta_1 = 1.3$ and $\Theta_2 = 1.95$

| gear | number of teeth | | $d_w$ | $b$ |
|---|---|---|---|---|
| | baseline[22] | var. ratio | mm | mm |
| input bevel pinion | 22 | 22 | 87.5 | 42.0 |
| input bevel gear | 80 | 80 | 318.0 | 42.0 |
| sun gear **C** | - | 23 | 54.6 | 46.6 |
| planet gear **C** ($q = 5$) | - | 26 | 61.7 | 46.6 |
| ring gear **C** | - | -77 | -177.9 | 46.6 |
| sun gear **D** | - | 31 | 71.4 | 34.7 |
| planet gear **D** ($q = 7$) | - | 17 | 39.2 | 34.7 |
| ring gear **D** | - | -67 | -149.8 | 34.7 |
| pump drive pinion | - | 43 | 114.4 | 22.4 |
| pump drive gear | - | 46 | 122.4 | 22.4 |
| motor drive pinion | - | 25 | 79.6 | 30.2 |
| motor drive gear | - | 46 | 146.4 | 30.2 |
| combining bevel pinion | 17 | 20 | 120.7 | 42.0 |
| combining bevel gear | 81 | 81 | 488.9 | 42.0 |
| sun gear | 62 | 87 | 249.7 | 81.5 |
| planet gear ($q = 5$) | 83 | 83 | 238.2 | 81.5 |
| ring gear | -228 | -253 | -726.1 | 81.5 |

Table 1: Basic design data of proposed transmission system

are obtained. In the two MPs, one of the variator shafts stands still and no power is transmitted via the hydraulic path. Since the whole propulsive power is transmitted mechanically, MPs are highly efficient operation conditions. CS modules are operated at transmission ratios

$$k_{ab} := \frac{\text{CS input RPM}}{\text{CS output RPM}} \tag{1}$$

between the two MPs. Therefore, the operation at mechanical points coincide with maximum resp. minimum MR speed. At $k_{ab} = \sqrt{\Theta_1 \Theta_2}$, the power flow in the variator path reaches a maximum. In principle, a CS module also can be operated at transmission ratios outside the interval of the MPs, but then idle power flow occurs which results in poor efficiency[33,15,23]. The minimum ratio of the CS modules of $1.3$ and the demanded rotor speeds of $180\,\text{RPM}$ to $285\,\text{RPM}$ ($70\,\%$ to $110\,\%$ of baseline main rotor speed) entailed changes in the combining bevel gear stage and the final planetary gear stage. For both, the numbers of teeth were adapted in order to reduce the stages' transmission ratios.

Design data of the tail rotor drive is not included in table 1 because it strongly depends on the available assembly space, shafts and bearings. However, at the present level of development, a fixed-ratio geartrain would not provide any additional insight. There is also no information on module/pitch, helix angle , addendum modification etc. of a gear. This is because of the fact that these parameters are the result of a comprehensive design process, which would go beyond the scope of this study.

As per assumption 4, the variator consists of two hydraulic machines. For the purpose of this study, axial piston motors with variable displacement produced by Bosch Rexroth[3] were used to model the properties of the variator. The basic machine data is presented in table 2.

| A6VE Series 71 | $P_{\text{corner}}$ kW | $T_{\text{max}}$ Nm | $n_{\text{max}}$ RPM | $\Delta p_{\text{max}}$ bar | mass kg |
|---|---|---|---|---|---|
| pump | 383.67 | 540.9 | 6773 | 450 | 28.26 |
| motor | 575.5 | 993.7 | 5530 | 450 | 51.91 |

Table 2: Estimated data of the required hydraulic motors[24]

The values were obtained by interpolating catalogue data to meet requirements of the UH-60's drivetrain[24]. The decisive factor is the corner power $P_{\text{corner}}$, i.e., the product of maximum torque and maximum angular velocity. This is caused by the fact, that when the transmission is operated in the first mechanical point, i.e., $k_{ab} = \Theta_1$, the pump stands still but has to counteract the input and output torque of the CS module and in $\Theta_2$ it rotates with no load, but at a maximum speed. For the motor, the situation is the other way around.

A combination of a pump and a motor, as it is in the variator, poses a hydrostatic transmission. Usually, the related hydraulic system is implemented as a closed circuit. This means,

that inlet of the pump is directly connected to the outlet of the motor and not to a tank. Owing to the principles involved, leakage occurs at hydraulic motors. In addition, the properties of the hydraulic fluid, such as density and viscosity, depend on temperature and pressure. They are also subject to ageing. As a consequence and to avoid cavitation at the suction side of the pump, additional measures such as feed pumps, a reservoir of hydraulic fluid and hydraulic accumulators will be needed. Since both hydraulic machines change their speed during operation and even stand still when the CS module operates at a MP, the feed pump cannot be combined with one of them as it is usually done. To guarantee a supply with hydraulic fluid in all operation conditions, the feed pump has to be driven by a shaft positively linked to the MR (similar to the lubrication pumps). A system containing all these items needs to be connected via appropriate hydraulic lines and reliable operation has to be ensured by valves (e.g., to limit pressure). Last but not least, the requirements on reliability may necessitate redundant hydraulic lines or even motors.

As mentioned earlier, the final design parameters of the transmission system are not yet defined. Furthermore, the approach leading to the presented layout was not intended to find a solution which satisfies all technical and economic demands but one which can be used to show the technical feasibility with as little changes compared to the proven baseline drivetrain as possible. A study on rotorcraft with variable speed main rotor in a mission context[11] yielded a permissible additional mass of 192 kg to 445 kg (424 lb to 980 lb). According to table 2, the four hydraulic motors of the variators weigh about 160 kg. So, a minimum of 30 kg remain for the hydraulic system, the gears of the CS modules and the changes to the mechanical parts of the drivetrain. However, the masses of the variators are estimations based on machines for mobile applications and a design for usage in rotorcraft may yield significant weight reduction. With state-of-the-art technology, the upper boundary of 450 kg of additional mass seems definitely achievable. Of course, there is still a lot of work to be done.

## 3. SIMULATION

To show the feasibility of a transmission system of the CS type in rotorcraft, a simulation model of the UH-60 was built up in Simulink[28] using Simscape Multibody™, a multibody simulation environment for 3D mechanical systems. It comprises a rigid fuselage with six degrees of freedom, main and tail rotor as well as the propulsions system with turboshaft engines and the drivetrain.

### 3.1. Methods

#### 3.1.1. Helicopter model

The main rotor is modelled using blade element theory. Each blade has 16 airfoil sections. Data on mass distribution[6,7] and 2-D data[27] of the lift and drag coefficients $C_L(\alpha, Ma)$ and $C_D(\alpha, Ma)$ are taken from the literature. A basic uniform inflow model[31] is used. The modelling of flap and lead/lag damping is based on published data[7,36]. To reduce simulation time, the tail rotor is modelled as a force acting on the TR hub. The required power is calculated from the induced velocity with a figure of merit of $\mathrm{FM_{TR}} = 0.75$[31]. It has to be pointed out, that this model is not intended to yield exact results on the aerodynamic behaviour of the rotor system, but is rather meant to give an estimation of the mutual interference of rotors and propulsion system.

The fuselage is a rigid body in the simulation. Data was taken from NASA Technical Memorandum 85890[14] and a manual[13]. Gross mass is assumed to be 7439 kg. Since this is a low value, low rotor speeds may be preferable[12]. In addition, lift and drag forces of the fuselage were calculated according to the formulae published by Yeo & Johnson[35] and Misté[17].

For the two General Electric T700 turboshaft engines the simplified open-loop dynamic model developed by Duyar et al.[9] was taken as a basis. It was obtained by combining linear state-space models determined at different operating points. To enable a more dynamic reaction to changes of the power turbine speed, the matrices building up the model were adapted to represent a sample time of 0.01 s instead of 0.1 s. This was achieved by linear interpolation between two consecutive states of the basic model.

#### 3.1.2. Model of transmission system

Gears and shafts of the transmission system are modelled as rigid bodies. The tooth meshes are considered ideal, i.e., tooth stiffness and losses are not considered in the model. The position of the inputs from the two turboshaft engines as well as the MR shaft are the same as in the baseline UH-60.

The changes to the drivetrain were implemented considering only the other parts of the drivetrain but no further restrictions of assembly space. As mentioned before, no layout for the TR drive was developed and so, the power flow to the TR is simulated by two ideal torque loads at the positions of the TR take-off. Each of them is equivalent to half of the power required by the TR in the given flight state. The shaft of the power turbine[32] is considered a part of the transmission system[6].

The variator is modelled by two Variable-Displacement Motors provided in the Simscape Fluids Library of Simulink. The information required for these blocks was taken from the data sheets of the chosen type of motor[4,3,5] and adjusted to the required corner power. The mechanical and volumetric efficiencies were calculated as functions of pressure drop, rotational speed and displacement acc. to Schlösser[25,26] with average loss factors and provided to the model as tabulated data. To reduce simulation time, the hydraulic system is kept as simple as possible. Only the hydraulic pipeline (including losses) and a pressure relief valve ($p_{\max} = 500\,\mathrm{bar}$) were simulated. The hydraulic fluid is considered as compressible and its properties were chosen to satisfy the requirements of the motor data sheets[4,3,5]. Feed pumps, redundant lines, etc. are neglected in the simulation model.

#### 3.1.3. Control

To achieve and maintain the flight states, the helicopter model needs some kind of control. The main rotor control angle is defined as

$$\vartheta_{\text{control}} = \vartheta_0 + \vartheta_{1c}\,\cos(\Psi) + \vartheta_{1s}\,\sin(\Psi), \tag{2}$$

where $\Psi$ is the azimuth angle. The three control angels $\vartheta_0$, $\vartheta_{1c}$ and $\vartheta_{1s}$ are governed by three PID controllers in such a way that the velocities in all spatial directions match the prescribed values. The TR thrust is also governed by a controller of this type. The rotational speeds of the turboshaft engines are governed by PID controllers, which keep the speed of the power turbines at a constant value of $20\,900\,\mathrm{RPM}$ by adapting the fuel flow. This is the first DOF of the transmission system, the second one is the transmission ratio of the variators. It is not governed in the model, but prescribed. This means, that the ratio of the displacements of the two hydraulic motors of the variator is a constant value. Since a given ratio can be achieved by an infinite number of pairs of displacements, the actual values are determined in such a way that the system pressure is at a constant $450\,\mathrm{bar}$. A recent study on a variable-ratio drivetrain for the UH-60[24] showed, that at this condition the transmission system is operated at maximum efficiency. However, there is a minimum value of displacement of each hydraulic machine. Near the mechanical points, i.e., when the motors are operated at low load resp. speed, the model of Schlösser reaches its limits and therefore these operation conditions are simulated by blocking the shaft of the pump (MP I) resp. the motor (MP II) and omitting the hydraulic system at all. However, since the properties of the hydraulic fluid and, as a consequence, the efficiency of the variator strongly depend on the temperature, a more sophisticated control system is needed in a market-ready helicopter. Finally, the question, whether the ratio is defined by the pilot or also governed by a controller is a challenging task for further research projects.

#### 3.1.4. Simualtion runs

To show the feasibility of a transmission system of the proposed design, the simulation was run at three different transmission ratios: in MP I, MP II and at $k_{ab} = \sqrt{\Theta_1 \Theta_2}$ (VarMax). Flight conditions are hover and forward flight with up to $40\,\mathrm{m/s}$.

### 3.2. Results

#### 3.2.1. General

The main outcome of the simulations is presented in this section. Speeds, power, pressure and flow are plotted in red, blue and green lines of different style acc. to figure 1. This styles are used throughout the section and in the interest of clear presentation, no legends are added to the individual plots.

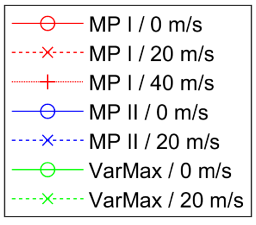


Figure 1: Line colours and styles

#### 3.2.2. Forward speed, main rotor RPM and power

The resulting forward speeds of all simulation runs are depicted in figure 2. In the first 15 seconds of the flights, the forward speed is in a satisfactory range

around the respective target values. However, the longer the simulations run, the more the speeds show an oscillating behaviour. This is caused by a lack of damping of the pitch, roll and yaw motion of the fuselage.

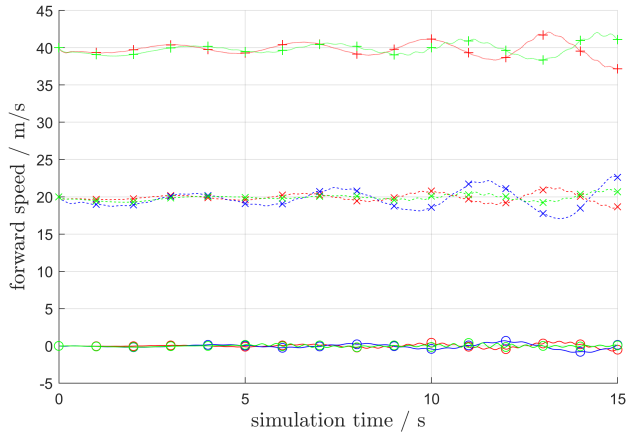


Figure 2: Time courses of horizontal flight speeds

The lateral and ascent/descent speeds are depicted in figures 8 and 9 in appendix A.2. Just like the horizontal speeds, the lateral velocities oscillate around the target value. The time courses of vertical speeds show considerable transient phenomena, but after about five seconds behave in the same way as the other velocities.

In figure 3 the time courses of MR speeds are presented. After transient processes MR speed at MP II is near the target value of about $19\,\mathrm{rad/s}$. Like for the horizontal speed, the graph of the forward flight case shows growing oscillation at the end of the simulation time. For the transmission ratio with the maximum variator power, the transient condition at the beginning is more significant due to the pressure build-up in the hydraulic system (cf. section 3.2.3). Afterwards, the target value of about $24\,\mathrm{rad/s}$ is maintained satisfactory. For MP I, i.e., maximum MR speed, the target value is $29\,\mathrm{rad/s}$. For forward flight with $40\,\mathrm{m/s}$, MR angular speed decreases after about ten seconds of simulation time. The reason for this can be explained with the calculated MR power demands depicted in figure 4.

Besides the power consumption of the MR, also the available intermediate engine powers of one resp. two turboshaft engines ($1150\,\mathrm{kW}$ resp. $2300\,\mathrm{kW}$) are plotted in figure 4. It can be seen, that for MP I and $40\,\mathrm{m/s}$ the power demand of the main rotor exceeds the engine limit, which leads to the decrease in angular velocity evident in figure 3.

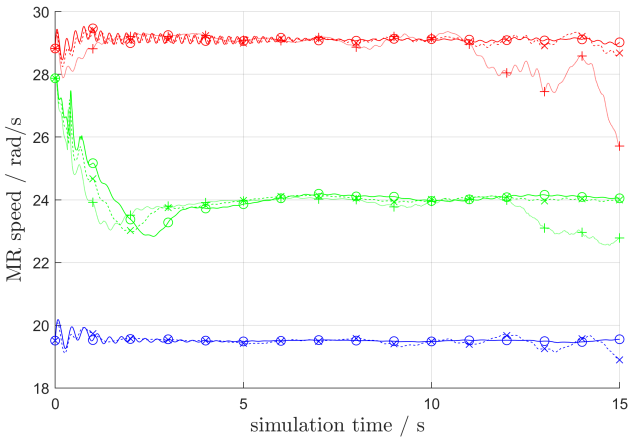


Figure 3: Main rotor angular speeds

For the other transmission ratios, the turboshaft engines are able to provide the required propulsive power. According to the results of the simulation, OEI operation is possible at low MR speed, i.e., high transmission ratio, and slow horizontal velocity resp. hover.

At this point a major shortcoming of the rotor and fuselage models used in the simulation manifests. At slow forward speed, one would expect a reduction of propulsive power compared to hover. In the contradiction to this, the simulation yields increasing power demands of the MR in slow forward flights. However, the results of the power calculation are sufficient for the purpose of this study.

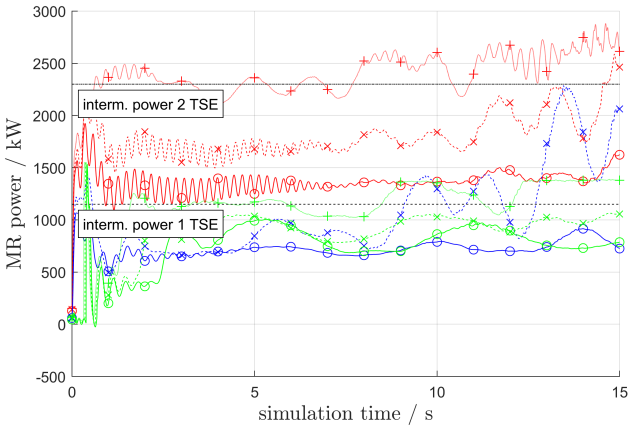


Figure 4: Time courses of MR powers

### 3.2.3. Variator

In this section flow and pressure in the variator are analysed for the case with maximum variator

power (VarMax). Figure 5 shows the courses of the flow of hydraulic fluid from the pump to the motor. Although the power demands of the MR differ, the flow is quite the same for all three forward speeds. This is caused by the fact that, although the displacements of the hydraulic machines are controlled in such a way to keep the pressure at 450 bar, there is a minimum displacement of 5 % of maximum displacement to ensure reasonable results of the variator's efficiency. This minimum is reached in all three flight conditions.

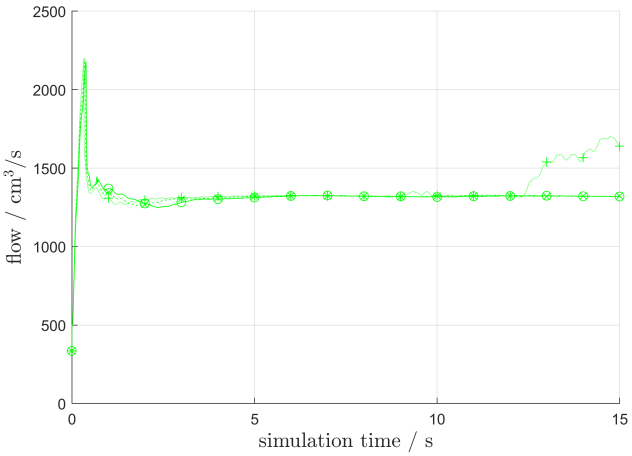


Figure 5: Flow of hydraulic fluid from pump to motor

As a consequence, the nominal pressure of the system cannot be reached. In figure 6 the time course of system pressures are depicted. Since the flow is nearly constant, they are similar to the courses of MR power demand. It can be seen, that the controller needs a long time to react to changes in pressure. In the 40 m/s case, the pressure reaches the upper limit of 500 bar two times and the pressure relief valve opens. The pressure increase also leads to a reaction of the controller and therefore an increased flow as can be seen in figure 6.

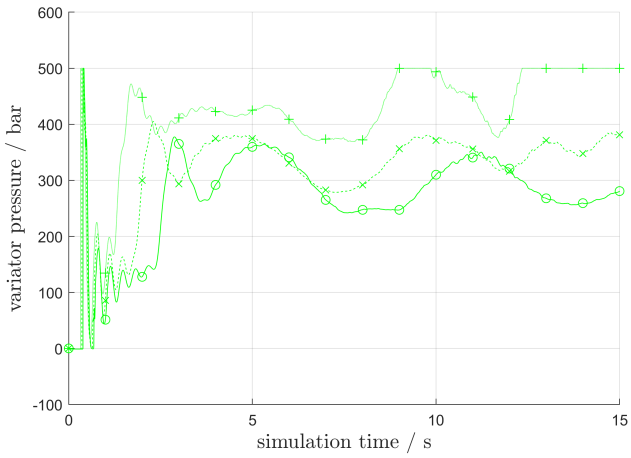


Figure 6: Pressure in hydraulic system

## 4. DISCUSSION

A basic design of a transmission system enabling variable main rotor speed whilst engines, tail rotor and accessories are not affected could be deduced. Its basic properties were used in time-domain simulations to show the feasibility of the technology in a helicopter similar to the UH-60. The results obtained for flight cases with low gross weight at slow forward speeds on sea level yielded satisfying results for power transmission and transmission accuracy. The rotor model used showed shortcomings in prediction of power demand. The shortage of a damping model for the fuselage and the immature flight controls negatively affected the results. However, it can be expected that these issues can be overcome.

Follow-up studies will address the found problems and will also extend the range of flight conditions with respect to gross weight, altitude and forward speed.

Future research on helicopters with variable main rotor speed will have to deal with the following questions:

- Does the introduction of the new technology has an impact on the reliability of the rotorcraft's propulsion system?
- How shall the main rotor speed be governed?
- Which changes can be applied to the rotor to improve the performance?
- How does the control system have to be adapted to limit the pilot's workload?

To answer them, a lot of development work and testing has to be done.

## A. APPENDIX

### A.1. Principal layout of transmission system

See next page.

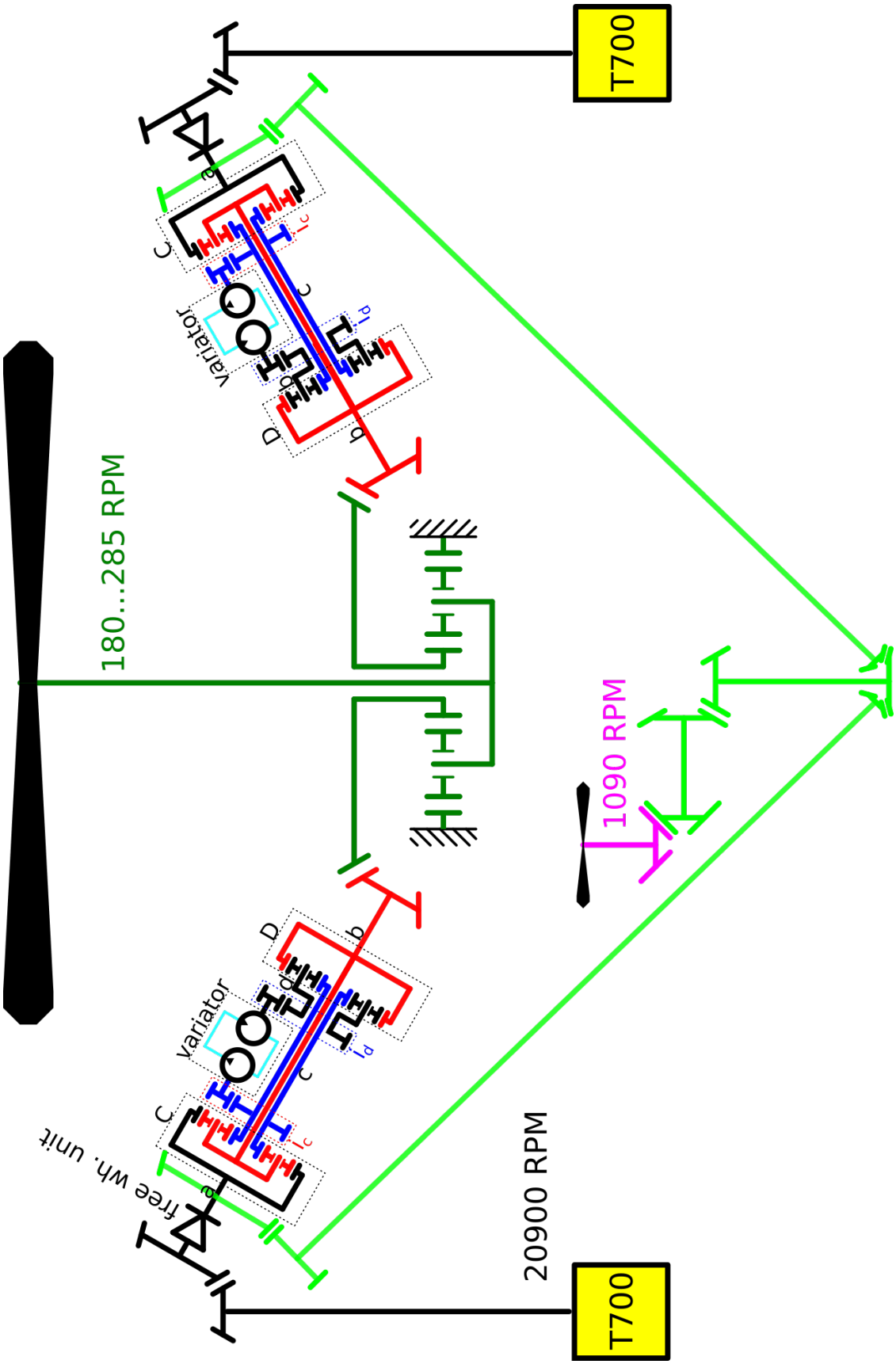


Figure 7: Pricipal layout of UH-60 transmission system with CS modules

### A.2. Additional results

Figures of lateral speed and ascent rate.

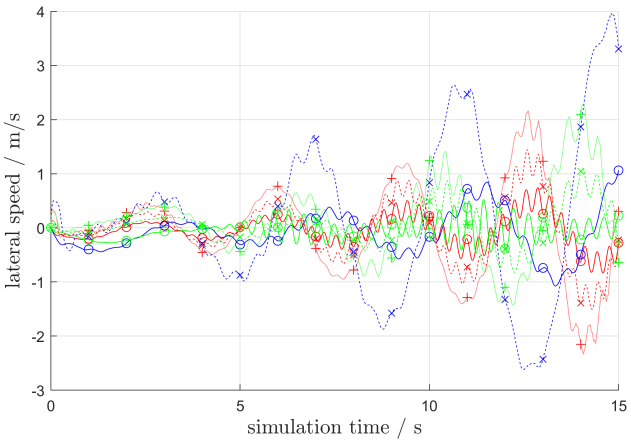


Figure 8: Time courses of lateral flight speeds

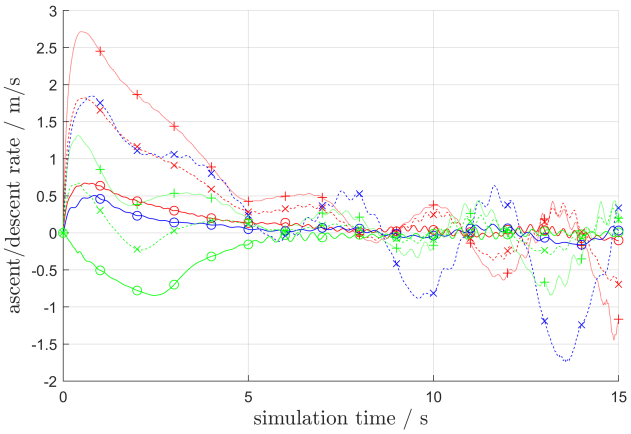


Figure 9: Time courses of vertical flight speeds

## REFERENCES


[1] H. Amri, P. Paschinger, M. Weigand, and A. Bauernfeind. Possible Technologies for a Variable Rotor Speed Rotorcraft Drive Train. In *42rd European Rotorcraft Forum 2016*, Lille, France, September 2016.

[2] Hanns Amri, Roland Feil, Manfred Hajek, and Michael Weigand. Übersetzungsvariable Getriebe für Drehflügler – Eine Notwendigkeit für künftige Hubschraubergenerationen? In *63. Deutscher Luft- und Raumfahrtkongress*, 2014. (In German).

[3] Bosch Rexroth AG Mobile Applications. *Variable Plug-in Motor A6VE: Data sheet Series 71*, 05.2016 edition. RE 91616/05.16.

[4] Bosch Rexroth AG Mobile Applications. *Variable Plug-in Motor A6VE: Data sheet Series 71*, 08.2015 edition. RE 91616/05.16.

[5] Bosch Rexroth AG Mobile Applications. *Variable Plug-in Motor A6VE: Series 65 and 71*, 10.2014 edition. RE 91616-01-B.

[6] Robert T. N. Chen. An Exploratory Investigation of the Flight Dynamics Effects of Rotor RPM Variations and Rotor State Feedback in Hover. NASA/Technical Memorandum 83726, NASA Ames Research Center, Moffett Field, California 94035-1000, September 1992.

[7] S. Jon Davis. Predesign Study For a Modern 4-bladed Rotor For the RSRA. NASA Contractor Report 166155, SIKORSKY AIRCRAFT DIVISION UNITED TECHNOLOGIES CORPORATION, March 1981.

[8] H. Dong and N.G. Barakos. Variable Speed Tail Rotors for Helicopters with Variable Speed Main Rotors. In *42nd European Rotorcraft Forum*, Lille, France, September 2016.

[9] Ahmet Duyar, Gu Zhen, and Jonathan S. Litt. A Simplified Dynamic Model of the T700 Turboshaft Engine. *Journal of the American Helicopter Society*, pages 62–90, October 1995.

[10] Harold Frint. Automated Inspection and Precision Grinding of Spiral Bevel Gears. Contractor Report Technical Report 4083, Sikorsky Aircraft Division United Technologies Corporation, Stratford, Connecticut, March 1987.

[11] W. Garre, H. Amri, T. Pflumm, P. Paschinger, M. Hajek, and M. Weigand. Helicopter Configurations and Drive Train Concepts for optimal Variable Rotor Speed Utilization. In *Deutscher Luft- und Raumfahrtkongress 2016*, Braunschweig, Germany, September 2016.

[12] W. Garre, T. Pflumm, and M. Hajek. Enhanced Efficiency and Flight Envelope by Variable Main Rotor Speed for different Helicopter configurations. In *42nd European Rotorcraft Forum 2016*, Lille, France, September 2016.

[13] HEADQUARTERS, DEPARTMENT OF THE ARMY. *OPERATOR'S MANUAL FOR UH-60A HELICOPTER, UH-60L HELICOPTER, EH-60A HELICOPTER*, 2009. TM 1-1520-237-10.

[14] Kathrin B. Hilbert. A Mathematical Model of the UH-60 Helicopter. NASA/Technical Memorandum 85890, Aeromechanics Laboratory, US Army Research and Technology Laboratories - AVSCOM Ames Research Center, Moffett Field, California, April 1984.

[15] Peter Hofmann. *Hybridfahrzeuge - Ein alternatives Antriebssystem für die Zukunft*, volume 2. Springer Wien Heidelberg New York Dordrecht London, 2014.

[16] Samuel A. Howard. Rotordynamic Feasibility of a Conceptual Variable-Speed Power Turbine Propulsion System for Large Civil Tilt-Rotor Applications. NASA/TM NASA/TM–2012-217134, Glenn Research Center, Cleveland, Ohio, July 2012. Prepared for the 68th Annual Forum and Technology Display (Forum 67) sponsored by the American Helicopter Society (AHS) Fort Worth, Texas, May 1–3, 2012.

[17] Gianluigi Alberto Misté. *Variable Speed Rotor Helicopters: Optimization of Main Rotor Turboshaft Engine Integration*. PhD thesis, Scuola di Dottorato di Ricerca in Ingegneria Industriale, 2015.

[18] Gianluigi Alberto Misté and E. Benini. Variable-Speed Rotor Helicopters: Performance Comparison between Continuously Variable and Fixed-Ratio Transmissions. *Journal of Aircraft*, 53(5):1189 – 1200, 2016.

[19] Gianluigi Alberto Misté, E. Benini, A. Garavello, and Gonzales-Alcoy Maria. A Methodology for Determining the Optimal Rotational Speed of a Variable RPM Main Rotor/Turboshaft Engine System. *Journal of the American Helicopter Society*, 60(5):032009–1 to 032009–11, July 2015.

[20] Mihir Mistry and Farhan Gandhi. Helicopter Performance Improvement with Variable Rotor Radius and RPM. *Journal of the American Helicopter Society*, 59:042010–10 to 42010–19, 2014.

[21] Andrew M. Mitchell, Fred B. Oswald, and Harold H. Coe. Test of UH-60A Helicopter Transmission in NASA Lewis 2240-kW (3000-hp) Facility. Technical paper, NASA, 1986.

[22] Fred B. Oswald. Gear Tooth Stress Measurements on the UH-60A Helicopter Transmission. NASA Technical Paper 2698, NASA, March 1987.

[23] P. Paschinger, H. Amri, K. Hartenthaler, and M. Weigand. Compound-Split Transmissions for Rotorcraft. In *43rd European Rotorcraft Forum 2017*, Milan, Italy, September 2017.

[24] P. Paschinger and M. Weigand. Study on possible solutions of a Compound-Split transmission system for the UH-60 helicopter (forthcoming). *Mechanism and Machine Theory*, 129:17–35, 2018. DOI: 10.1016/j.mechmachtheory.2018.07.004.

[25] W.M.J. Schlösser. Über den Gesamtwirkungsgrad von Verdrängerpumpen. *Oelhydraulik und Pneumatik*, 12(10):415–420, 1968. (In German).

[26] W.M.J. Schlösser. The Overall Efficiency of Positive Displacement Pumps. In *Fluid Power Symposium*, January 1969.

[27] Daniel P. Schrage, Paul W. Losier, Liu Shoe-Shen, Sriprakash Sarathy, and Jerry P. Higman. The Assessment of the Capabilities and Limitations of the Flight-Lab Simulation Software in the Prediction of Rotorcraft Component Loads to Support Flight testing. Contract Report N00421-94-M-3691, Georgia Institute of Technology, September 1995.

[28] Simulink. *Version 9.0 (R2017b)*. The MathWorks Inc., Natick, Massachusetts, USA, 2017.

[29] C. A. Snyder and C. W. Jun. Acree. Preliminary assessment of variable speed power turbine technology on civil tiltrotor size and performance. In *American Helicopter Society 68th Annual Forum*, 2012.

[30] United States Army Aviation Warfighting Center, Fort Rucker, Alabama. *UH-60A STUDENT HANDOUT : UH-60A Powertrain/ Rotor System*, February 2008.

[31] Berend Gerdes van der Wall. *Grundlagen der Hubschrauber-Aerodynamik*. Springer-Verlag Berlin Heidelberg 2015, 2015. (In German).

[32] Mahesh Kumar Varrey. FEASIBILITY STUDY OF T700 ROTORCRAFT ENGINE ROTOR SUPPORTED BY HYBRID AIR FOIL BEARINGS. Master thesis, The University of Texas at Arlington, 2011.

[33] Weihua Wang, Ruifang Song, Mingchen Guo, and Liu Songshan. Analysis on compound-split configuration of power-split hybrid electric vehicle. *Mechanism and Machine Theory*, 78:272–288, 2014.

[34] G. E. Welch. Assessment of Aerodynamic Challenges of a Variable-Speed Power Turbine for Large Civil Tilt-Rotor Application. In *American Helicopter Society 66th Annual Forum*, 2010.

[35] H. Yeo and W. Johnson. Performance Analysis of a Utility Helicopter with Standard and Advanced Rotors. *Journal of the American Helicopter Society*, pages 250–270, July 2004.

[36] H. Yeo and W. Johnson. Comparison of Rotor Structural Loads Calculated Using Comprehensive Analysis. In *31st European Rotorcraft Forum*, 2005.